JOURNAL OF Applied Polymer SCIENCE

Structure and Morphology of Linear Polyethylene Extrudates Induced by Elongational Flow

Frantisek Rybnikar,[1] Martina Kaszonyiova,[1] Roman Cermak,[2] Veronika Habrova,[3] Martin Obadal[4]

[1]Department of Production Engineering, Tomas Bata University in Zlin, Zlin, Czech Republic

[2]Department of Polymer Engineering, Tomas Bata University in Zlin, Zlin, Czech Republic

[3]Polymer Institute, Brno, Czech Republic

[4]Borealis Polyolefine GmbH, Linz, Austria

Correspondence to: M. Kaszonyiova (E-mail: mhribova@ft.utb.cz)

ABSTRACT: This study focuses on the structure, morphology, and properties of linear polyethylene (PE) profiles manufactured by continuous extrusion. High level of chain orientation was achieved using specific flow and processing conditions. An extrusion die with semihyperbolic convergency was used to generate high percentage of elongational flow and chain extension. Simultaneously, high extrusion pressure and relatively low melt temperature led to flow-induced crystallization of PE extended chains. The structure of PE tapes consists of crystal aggregates with different level of orientation and crystallinity. © 2012 Wiley Periodicals, Inc. J. Appl. Polym. Sci. 000: 000–000, 2012

KEYWORDS: morphology; extrusion; crystallization; polyolefins

Received 27 March 2012; accepted 4 July 2012; published online
DOI: 10.1002/app.38323

INTRODUCTION

Many properties of important commercial plastics, such as polyolefins can be improved by a preferential molecular orientation. There are several orientation types and procedures. The polymer can be oriented in one, in two or more directions. The orientation process may proceed from solution, melt or solid state mainly above glass transition temperature (T_g) and below melting temperature (T_m). Polymer chains are oriented to a distinct orientation degree in the strain direction(s). Orientation process can be performed using different techniques. Stretching the chains in the solid state under action of tension forces has been a common way to produce high-oriented films and fibres. This process, called orientational drawing, was studied in detail by several research groups.[1–4] Unfortunately, it cannot be used for large volume profiles. Moreover, products manufactured in this way have very often surface defects. Song et al.[5] also mention other special solid state techniques, such as ram or hydrostatic extrusion, but these processes are very slow. The orientation process directly in the polymer melt has been also studied.[6–9]

From rheological point of view, the melt state deformation is appealing and several studies have been focused on device construction and on modeling best flow geometries for production of high-oriented articles.[7,9–14] The application of this self-reinforcement in the injection molding process and continuous or discontinuous extrusion has been of particular interest and the tendency in searching the processing conditions and using specific geometries has been similar. McHugh[6] reported that elongational forces in the flow contribute to the chain orientation and fibrils formation more than shearing forces. Therefore, scientists have been seeking the geometry leading to high percentage of elongational flow. The conical die in the case of discontinuous [see Refs. 7–9] and continuous extrusion[10–14] and also a conical injection nozzle in case of injection molding[15] were found to be applicable for self-reinforcement.

The conical dies and nozzles provided acceleration of the melt which was sheared and elongated in addition under specific processing conditions. High pressure and relatively low sample temperature played marked role in this orientational effect. The self-reinforced products showed improved mechanical and thermal properties and their morphology was fibrillar or consisted of shish-kebabs. However, in agreement with theory, the conical type of convergency did not provide pure elongational flow, necessary for more perfect chain arrangement, and therefore better properties.

According to Pendse and Collier,[16] the pure elongational flow should be obtained using semihyperbolic convergency. Nevertheless, except for our research group, no one has used this

Table I. Extrusion Processing Parameters and Sample Characteristics

No.	Samples	MFI (190°C, 2.16 kg), g/10 min	Extrusion pressure (MPa)	Temperature of converging channel, (°C)	Temperature T_1, (°C)	Temperature T_2, (°C)	Density, g/cm^3
1	BH-5363	6.5	16.5	190	190	190	0.9533
2	Liten TB 38	0.55	16.4	180	180	170	0.9544
3	Liten TB 38	0.55	58.6	145	125	120	0.9587
4	Liten TB 38	0.55	52.5	145	115	110	0.9575
5	BH-5363	6.5	60.0	145	126	121	0.9607
6	BH-5363	6.5	63.1	145	125	120	0.9630

convergency effect for the continuous extrusion, which can be, in contrast to use of capillary rheometer, more popular for industry.

Therefore, within our previous work, experimental extrusion line with specially designed extrusion die, equipped with semi-hyperbolic round or rectangular channel and several heating/cooling fixing zones, was constructed.[17] Round and rectangular channel cross-sections were designed on purpose as a basic rheological geometry. Using this line, high-oriented polyolefin rods with improved properties compared to extrudates, produced by ordinary extrusion conditions, were prepared.[18] This article focuses on preparation of high-oriented polyethylene (PE) tapes with cross-section of approximately 2 × 20 mm^2 and description of their structure, morphology, and properties.

EXPERIMENTAL

Materials

Two commercial linear (high density) PEs, Liten TB 38 (Chemopetrol, Litvinov, Czech Republic), with melt flow index (MFI) 0.55g/10 min (190°C, 2.16 kg, ISO 1133), density 0.9544 g/cm^3 (ISO 1183) and Borealis BH 5363 (Borealis A/s Kongens Lyngby, Denmark) with MFI 6.50g/10 min (190°C, 2.16 kg) and density 0.953 g/cm^3 were used in this study.

Samples

For measurements 20 mm long, parts of band extrudates (15 mm wide and 2 mm thick) were used. The sample characteristics and preparation conditions are summarized in Table I.

Extrusion

A conventional Brabender single-screw extruder (Brabender OHG Duisburg, Germany) with diameter D 30 mm and length $L = 25$ D was used to produce extrudates of rectangular cross-section (tapes). The extruder was implemented by a Zenith PEP II gear pump 1.2 cm^3/rev (Zenith Pumps, Sanford, NC) generating high pressure and a novel extrusion die with semihyperbolic convergency and a rectangular outlet of 2 × 20 mm^2. The die was designed to achieve self-reinforcement, that is, to produce high-oriented profiles. Two basic prerequisites were realized: (1) high percentage of elongational flow was assured by a converging channel and (2) precisely controlled cooling of the extrudate at the outlet of the converging channel was secured by two separately controlled heating/cooling zones (T_1, T_2). Scheme of extrusion line is shown in Figure 1(a). The die picture and development of the flow in die are described in paper.[18]

To improve slip between die and polymer and to decrease the probability of plug formation in the die, the production of tapes was started after extrusion of approximately 1 kg of low-density PE.

X-ray Scattering

Crystal structure, crystallinity, and sample orientation were characterized by wide-angle X-ray diffraction (WAXS) and small-angle X-ray diffraction (SAXS). The wide-angle diffraction was measured in the 2Θ range 3–39° using HZG diffractometer with line-shaped beam of CuK$_\alpha$ Ni-filtrated radiation. Measuring step size 0.03° 2Θ and time 5 s were used. Measurements were performed in sample direction *a*–along and *b*-perpendicular to extrusion direction [Figure 1(b)]. Transmission and reflection modes were used, where the intensities differed slightly but the trend was identical. For small angle (SA) scattering (SAXS), Rigaku-Denki goniometer with slit collimation was used. The measuring conditions were: 2Θ range 0.08–1°, step size 0.01°, time 50 s. The equipment enabled to measure the regular periodic formation still to 800 Å. SAXS measurement was not corrected on the influence of smearing given by linear X-ray source. Therefore, the real values of SAXS periodicity (LP) can be lowered by about 10–20%. The amount of amorphous phase (A) was calculated as the area ratio of the amorphous halo at 2Θ = 19.5° and total sample (amorphous and crystal) diffraction. Figure 2 shows the diffraction scan with peaks resolved to individual components. The crystallinity (X) was calculated as the ratio of crystalline and total diffraction areas.

The peak intensities (I_c) of diffracted scans were corrected for sample thickness and dimension. The sample crystal size (L_{110})

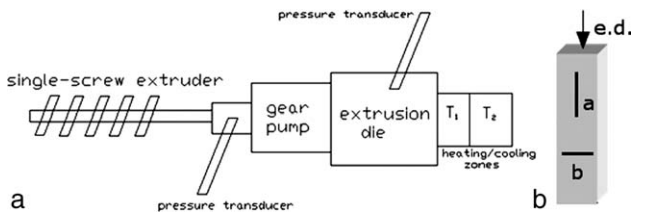

Figure 1. (a) Scheme of the production line, (b) X-ray measuring directions; a—along to an extrusion direction (e.d.), b—perpendicular to an extrusion direction.

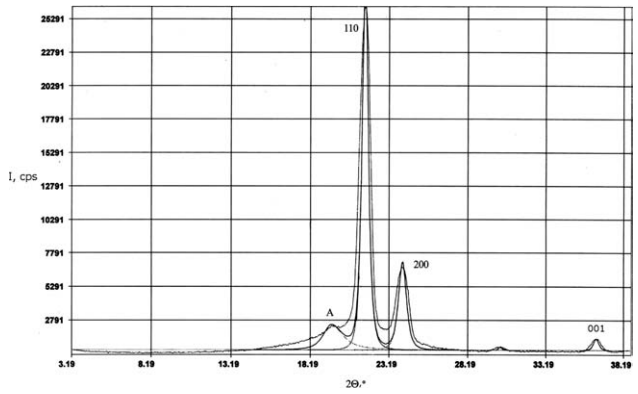

Figure 2. X-ray scan of the sample 6 with resolved peaks 110, 200, 001, and amorphous halo.

was calculated from the 110 crystal diffraction peak profiles according to the Scherrer equation.[19] As a standard "perfect" crystal terephthalic acid with the peak at $2\Theta = 17.4°$ and the half maximum breadth 0.3° 2Θ was chosen.

Orientation degree O_r was characterized by the azimuthal 2Θ angle where the original peak 110 intensity on the equator decreased to one half.

Electron Microscopy

The sample morphology was characterized by transmission electron microscopy (TEM—Tesla BM 500, Tesla Brno, Czech Republic) and scanning electron microscopy (SEM—Jeol JSM-35, Jeol, Japan).

The replicas of selectively etched sample surfaces were studied using Tesla BM 500 transmission electron microscope. The sample etching was performed by 1% solution of $KMnO_4$ in 85% H_3PO_4 at 25°C. The etching time was 10 min. The samples were shadowed by a thin Au or Pt layer. The sample replica was reinforced by evaporated carbon layer. For replication, 10% water solution of poly(vinyl alcohol) was used. The magnification on TEM micrographs shows 1 μm bar.

Samples for SEM were selective etched as above and covered by a thin gold layer in a sputter device. The fracture surfaces of extrudates in liquid N_2 were also observed.

Differential Scanning Calorimetry

Melting properties of the samples were measured using Perkin-Elmer Pyris I (Perkin Elmer) differential scanning calorimeter. Samples of approximately 5 mg were cut from the tapes. Heat flow was 10°C/min in the temperature range 50–150°C in the nitrogen atmosphere. From the melting endotherms, sample melting temperatures (T_m) and heats of fusion (ΔH) were evaluated. Sample crystallinity (X_{DSC}) was calculated from heat of fusion of the sample (ΔH) and heat of fusion of 100% crystalline polymer ($\Delta H_0 = 293$ J/g according to Refs. 20,21).

Mechanical Testing

Mechanical properties were measured by a Zwick Z 020 (Zwick Roell, Italy) tensile tester equipped with external extensometer. The extensometer with the gauge length 20 mm was used to obtain precise values of elastic moduli. The tapes 70 mm long were stretched at room temperature and elongation speed 10 mm/min.

Due to sample slippage in mounting clamps, the measurement of mechanical properties was supplemented by dynamic mechanical analysis (DMA) performed by a DMA 2980, dynamic mechanical tester (TA Instruments). The extruded tapes were tested in a single cantilever bend mode. Dynamic sinusoidal cycling of the stress with the amplitude of 15 μm and frequency of 1 Hz was applied in the temperature range of 30–100°C at the heating rate of 2°C/min. The samples for DMA were prepared by cutting the tapes into two parts along the extrusion direction. The gauge length of the sample was 25 mm.

Table II. Crystal Structure and Morphology of Oriented Bands of Linear Polyethylene

Sample	Measuring direction	110, 4.09 Å I_c $\times 10^{-3}$, cps	a/b	200, 3.7 Å I_c $\times 10^{-3}$, cps	a/b	Peak 110 width 2Θ°	L_{110}, Å	O_r,°	A ± 2, %	Morphology EM, Å	SA, Å
1	a	29	1.3	20	1.5	0.42	294	50	21.8	L 200-500	280
	b	23		13		0.44	281		23	P 2000-6000	
2	a	25	2.2	17	2.8	0.44	281	40	19	B 300	360
	b	11		6		0.48	242		23	L 200-500	
3	a	45	2	21	1.4	0.42	294	30	23		350
	b	23		15		0.44	281		27		
4	a	50	3.8	37	12.3	0.46	258	25c	23.8	L 200-300	350
	b	13		3		0.46	258		25.6	P 1000	
5	a	138	42	30	23	0.45	269	6	14.3	B	370
	b	3.3		1.3		0.48	242		40d	P	
6	a	170	57	33	16	0.44	281	7	13.5	B 200-300	350
	b	3		2.1		0.48	242		71d	P 500	

I_c, peak intensity; O_r, orientation degree; L, lamella; P, band structure; B, blocks; a, along extrusion direction; b, perpendicullar to extrusion direction; c, I_{110} peak divided in two peaks ± 30°off equator; d, due to voids between fibrils.

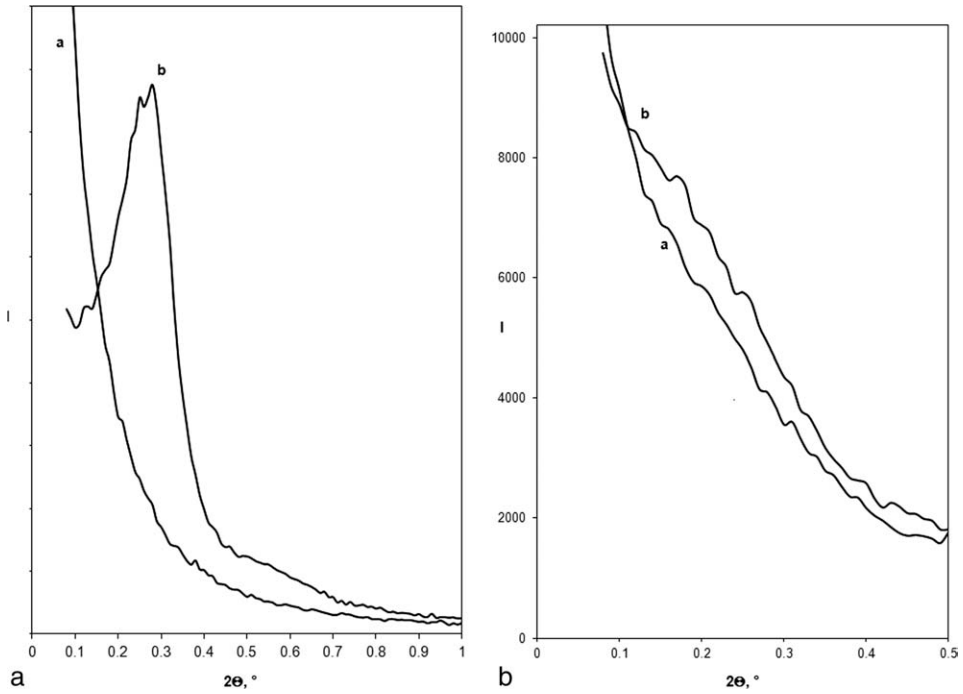

Figure 3. (a) SAXS scans of oriented sample 6 with maximum in *b*-direction. (b) SAXS scans of nonoriented sample 2 measured in *a*- and *b*-directions.

RESULTS AND DISCUSSION

Structural Observation

X-ray Scattering

WAXS. All samples crystallized in the stable orthorhombic crystal lattice were characterized by the most intensive reflections 110 (d = 4.09 Å), 200 (d = 3.7 Å), and 001 (d = 0.25 Å). Besides of the crystal peaks, a diffuse amorphous halo (A) was situated at 19.5° 2Θ of the scan (Figure 2). The crystal lattice parameters were similar in all samples which means that they were not influenced by the orientation process. Peak intensities (I_c) on equator varied strongly depending on sample and measuring direction (Table II). Depending on growing orientation degree, the I_c values increased in accord with growing orientation of polymer chains in *c*-axis direction. The crystal size L_{110}, based on 110 peak width and calculated using Scherrer equation,[19] was not much different (244–294 Å) for all samples and both measuring directions. The L_{110} values were slightly lower than SA periods measured in *b*-direction.

One of the most important characteristics of oriented samples is their orientation degree. Here, we characterize the orientation degree by three characteristics:

(a) Sample 110 peak intensity (I_c) on equator: it grows with orientation degree.
(b) a/b ratio of the peak intensities in measurements in *a* and *b* direction: it grows with orientation degree.
(c) The azimuthal peak angle where the peak intensity decreases to ½ ($I_{0.5}$): it decreases with sample orientation degree. The data were obtained from radial measurements, when the sample was oriented to measuring direction in angles 0, 10, 20, and 90°.

The trend of all orientation degree characteristics is similar in all samples. Table II shows the degree of orientation by these characteristics for samples 1–6. Preliminary evaluation of orientation degree was made by X-ray film technique. From the measured values of orientation degree, it is possible to divide the samples in three groups:

1. low oriented (1,2,3)
2. medium oriented (4)
3. high-oriented (5,6)

Regarding sample 4, we have to take in mind that the equatorial I_c values shown in Table II do not represent the maximal peak height which lies at ca ± 30° of the equator.

Orientation degree values were in reasonable agreement with other methods used for evaluation of molecular orientation. The measurement in *a*-direction gives information only about the level of crystal orientation in this direction, that is, in the direction of molecular chains. In case of low-oriented samples, the structure should be practically isotropic in all directions. The comparison of I_c values measured in *a*- and *b*-direction shows that there is difference among samples due to sample orientation. The amorphous content of low- and medium-oriented samples was in the range 19–27%, lower in *a*– direction, in high-oriented samples, %A decreased to about 14% in *a*- measuring direction but increased substantially in *b*-direction due to void and holes. The % of amorphous peak A in Table II shows, however, that isotropy found in *a*-direction need not be identical in different measuring direction. It evidences that amorphous phase can be also oriented. Understandably, extrusion technology essentially leads to slight orientation at least in skin layer. It

is clear from Table II that degree of an arrangement and orientation of crystal and amorphous phases differ according to measuring direction. The prerequisite of isotropic morphology is fully filled only in case of sample 1, where the content of amorphous phase is virtually same and independent on measuring direction and partly valid in case of samples 2, 3, and 4. The sample 4 partly differs from previous ones because it represents transient type of orientation, when crystallites are oriented in two directions. In case of samples 5 and 6, we can see that the amorphous phase is more distinct in *b*- than in *a*-direction.

Finally to sum up WAXS transmission results, the observed samples can be divided according to orientation level into three basic groups: practically non- or low-oriented samples (1–3), medium-oriented samples (4) and high-oriented extrudates (5 and 6) showing self-reinforced effect. Crystal width and corresponding L_{110} values did not differ much for all samples or measuring directions *a, b.* The crystal size was in the range 242–294 Å. The values of small-angle period (SA) had the same trend as L_{110}, only the SA values were slightly higher (280–360 Å). In view of Table I, it can be said that special flow and processing conditions can increase sample orientation degree of used material having optimal melt flow characteristics.

SAXS–Transmission Mode. The SAXS data confirmed presence of high-oriented periodic structures which are usually attributed to thickness of lamellar systems. Several forms of small-angle diffractograms were observed in our study. First, on the *b*- scan, a shoulder or marked maximum indicated different perfections of the periodic structure (see Figure 3(a)]. Second, it was noticed a continuous scattering curve with decreasing intensity, typical for nonoriented system [see Figure 3(b)]. The diffraction scans with a shoulder or maximum were found only in *b*-measuring direction. Measurement in *a*-direction proved no periodicity in the molecular chain direction at least with dimensions below 800 Å. The periodicity greater than 800 Å in *a*-direction was not observed even by electron microscopy. Nevertheless, the important finding is similar periodicity at about 350 Å in *b*-direction. Regarding the measurement in *b*-direction, the marked maximum or shoulder was observed in case of high-oriented samples. On the other hand in *a*-direction, the maxima were missing. Practically, same value of small-angle periodicity approximately 350 Å in case of high- or medium-oriented samples means that structural elements with identical size formed during orientation. This fact is logical because the high unidirectional oriented sample structure formed under similar processing condition (pressure and temperature range). Easy formation of voids and cracks in PE samples can be explained by a small lateral coherence of parallel fibrillas which are bond by only weak intermolecular forces without substantial physical entanglement.

In general, X-ray measurements confirm that oriented crystal structure is organized in different levels with *c* molecular axis in sample orientation direction. The size of crystal in the L_{110} direction lies in the narrow range (242–294 Å) and is relatively independent on sample type or measuring direction. It is slightly lower than the SA periods. The organization of *b*-axis into direction perpendicular to the *a*-direction is random. Periodicity in ***b***-direction shows that fibrils are practically commensurate with the width approximately 350 Å.

Electron Microscopy

The selectively etched surface of extruded samples is observed by SEM and TEM. The morphology reflected the sample orientation degree. The low-oriented sample 1 (Figure 4(a)] is characterized by individual twisted lamellae (Ø 300–500 Å) without any preferred orientation (SEM insert). The 300–500 Å dimension corresponds to the range of lamellar thickness. The detailed TEM picture in Figure 4(a) suggests that the lamellar system belongs to slightly deformed lamellar spherulites (L). The individual lozenge-type thin lamellae (350–400 Å thick and 1–2 μm long) are piled to twisted stacks (s).

In sample 2, the spherulite is slightly deformed [Figure 4(b)]. In some places, the spherulites fully changed to parallel extended lamellar fibrils (F) mostly oriented in extension direction (arrow). In some areas fibrils bend (b) even in the opposite direction for a short distance (marked l). Besides prevailing fibrils there are seen remnants of original spherulite lamellae and microvoids (v) (0.1–0.2 μm) and cracks (0.4–0.8 μm) marked c.

Micrographs of the sample 3 in the Figure 4(c) show that the sample morphology is still not unified. Besides deformed spherulite structure appears a new type called "shish-kebabs" (sb), the system of straight parallel extended fibers 0.7–1.4 μm apart with short adjacent perpendicular branches 0.2–1.2 μm long.

Structure of sample 4 [Figure 4(d)] represents a very dense strict and parallel shish-kebabs, where the short branches are 0.3–0.4 μm long and 700–800 Å thick. The fibrils break mainly in a brittle fashion (r in SEM insert).

The samples 5 and 6 are characterized by a almost identical morphology as is apparent from Figure 4(e, f). The structure consists of parallel fibrils of extended shish-kebabs with shorter and thicker branches [Figure 4(f)]. In the parallel fibrillar system are also cracks [marked by c in Figure 4(e)] forming voids that are partially filled with longer more separated and twisted side branches of the shish-kebab (marked by T).

Figure 4(g) shows the fractures surface of the sample 6 where the some morphological features are apparent: thick fibrils (F), individual extruded lamellae (L), voids (V), or cracks (C).

Properties Measurements

Differential Scanning Calorimetry. The typical DSC heating scans are shown in Figure 5. The pertinent data for melting temperature T_m, heat fusion, and crystallinity are summarized in Table III. The melting process of all samples is characterized by a single broad melting peak close to 130°C. The peak area and peak maximal temperatures differ slightly for each sample and its orientation degree. Samples 5 and 6 with the highest O_r have the T_m values 2–3°C higher than the less-oriented samples 1–4. Similar situation is valid for the heat of fusion and corresponding crystallinity data. The crystallinity data measured by three different methods, density, DSC, or X-ray diffraction, naturally differ but their trend is identical, the two highly oriented samples 5 and 6 clearly differ from the less oriented.

Applied Polymer SCIENCE

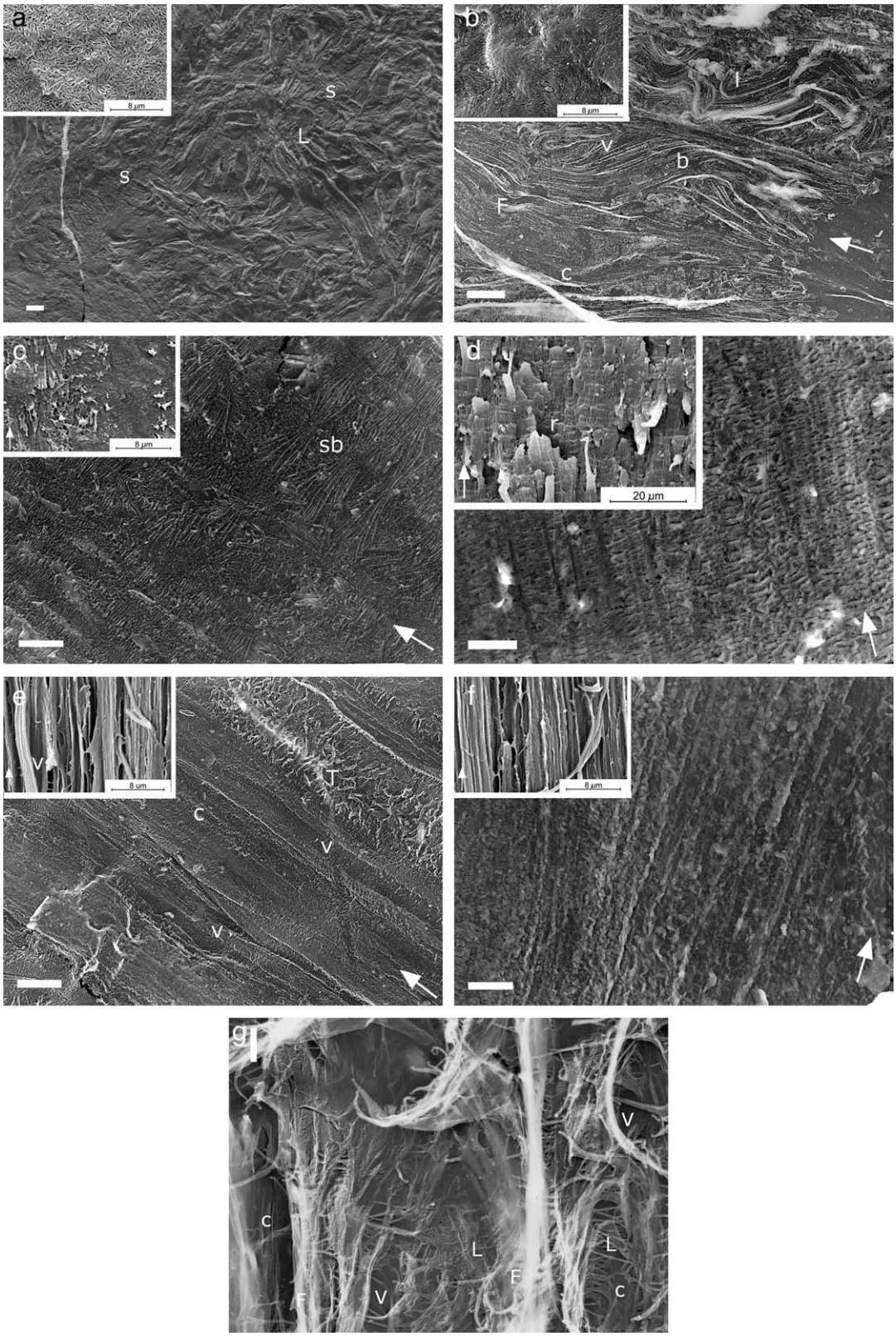

Figure 4. TEM and inserted SEM micrographs of (a) sample 1, (b) sample 2, (c) sample 3, (d) sample 4, (e) sample 5, (f) sample 6, (g) TEM micrograph of sample 6, fracture surface.

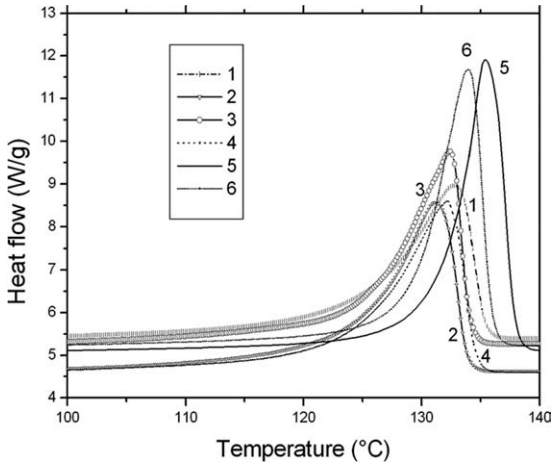

Figure 5. Melting endotherms of extrudates.

Mechanical Properties

As it is evident, the self-reinforcement can lead to extrudates with increased crystallinity and preferred molecular orientation to different mechanical properties, mainly high strength. Unfortunately, the sample character has not allowed precise evaluation of tensile properties. Due to sample slippage in mounting clamps, it was not possible to measure tensile strength; only elastic modulus could be evaluated. The results are in Table IV. As can be seen, the tapes supposedly self-reinforced (number 5, 6) show higher elastic modulus compared to less-oriented extrudates (sample 1–3). Nevertheless, tensile behavior of the ordinary and oriented samples can be compared.

Due to problems with slippage, the samples were tested also using DMA analysis in single cantilever bend mode. It seems to be more suitable method for mechanical properties evaluation of self-reinforced samples. Moreover, this analysis enables also to assess the dependence of the mechanical properties on the temperature. The dependence of storage modules on temperature which is related to the stiffness and also thermal stability is the most important result. From plots of bend storage modulus as a function of temperature displayed in Figure 6, it is evident that the storage modulus in all cases decreases relatively fast with increasing temperature in the whole observed region. However, an approximately threefold enhancement of the storage

Table III. DSC Melting Characteristics

Sample	Melt temperature T_m (°C)	Heat of fusion ΔH_m (J/g)	X (%) DSC	Density	X-ray
1	132.8	182	62.3	68	77
2	131.3	189	64.5	69	78
3	132.5	188	64.2	72	78
4	132.2	193	65.8	71	78
5	135.5	199	68.1	73	86
6	134.0	198	67.5	75	87

% crystalline PE = 1000 g/cm^3, amorphous 0.855 g/cm^3.

Table IV. Mechanical Properties, *a*-direction

Sample	Tensile E-modulus (MPa)—tapes	DMA—Bend storage modulus (MPa) at 30°C	at 100°C
1	980	3050	590
2	920	2800	450
3	1360	3900	860
4	1780	5390	1160
5	2500	9210	2860
6		8130	3530

modulus at 30°C can be observed in the case of the high-oriented samples in contrast to the sample extruded under common processing conditions (compare sample 1 and 5 or 6 in Table IV). In addition, the storage modulus value of the high-oriented sample measured at 100°C is almost equal to the modulus value of the ordinary sample measured at 30°C. This fact indicates excellent mechanical properties of the extrudates with high level of orientation prepared from materials 5 and 6 under processing conditions leading to self-reinforcement. Regarding the samples number 3 and 4 produced also under special extrusion conditions but from material with higher molecular weight, DMA results, similarly to previous measurements, show that in this case, the orientation effect was not as intensive as for lower molecular weight material. The storage modulus of the extrudates number 3 measured at 30°C was approximately double, and modulus of the sample number 4 even lesser than double, compared to the sample 1.

With respect to mechanical properties of PE tapes, it can be summarized that they can be improved using our production line under special flow and processing conditions. Moreover, to produce really high-oriented articles, also the proper type of material must be used. The middle molecular weight types of high-density PE seem to be more suitable than the low molecular weight ones.

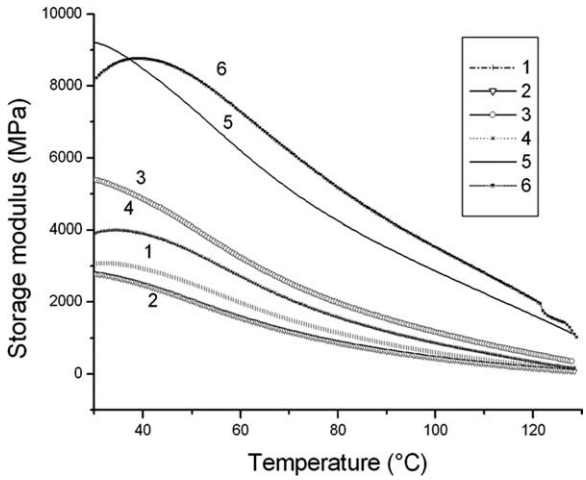

Figure 6. DMA curves of extrudates.

SUMMARY

This article presents the study of the structure, morphology, and properties of PE tapes extruded using semihyperbolic extrusion die providing high percentage of elongational flow.

A system of mainly parallel fibrils or ribbons which consists of orthorhombic crystals with *c*-axis oriented into *a*- sample extrusion direction characterizes the sample morphology. The data from Tables I and II and Figure 4 show that high orientation level depends on several factors: high extrusion pressure (about 60 MPa), relatively low processing temperature (channel T = 145°C, T_1 = 125°C, and T_2 = 120°C). A greater tendency to higher orientation degree was observed in case of samples with lower molecular weight (higher MFI). Fibrils or ribbons with thickness of 6000 Å consist of periodic layers with thickness of about 350 Å. This periodicity leads to occurrence of pronounced meridional maxima in SAXS scans. In other directions, regular orientation of lamellar structure was not observed. High-oriented extrudates showed, due to their morphology, higher crystallinity and melt temperature. Compared with low-oriented extrudates, the high-oriented samples prepared by self-reinforcing technology have several folds higher storage modulus measured in wide temperature range.

The amorphous content of non- or low-oriented samples was in the range 18–20% and decrease to a ca 12% in highly oriented samples 5 and 6 in *a*-direction and increased due voids and crack effect in *b*-direction.

ACKNOWLEDGMENTS

This research was financially supported by the Czech Ministry of Education, Youth, and Sports in the R&D project under the title 'Modelling and Control of Processing Procedures of Natural and Synthetic Polymers', No. MSM 7088352102 and 'CEBIA Tech', No. CZ.1.05/2.1.00/03.0089.

REFERENCES

1. Peterlin, A.; Ingram, P.; Kiho, H. *Makromol. Chem.* **1965,** *86*, 294.
2. Korsukov, V. E.; Marikhin, V. A.; Myasnikova, L. P.; Novak, I. I.; *J. Polym. Sci. Part C: Polym. Symp.* **1973,** *42*, 847.
3. Myasnikova, L. P. *Plast. Kautsch.* **1986,** *33*, 121.
4. Elyashevich, G. K.; Karpov, E. A.; Kudasheva, O. V.; Rosova, E. *Mech. Time-Depend. Mater.* **1999,** *3*, 319.
5. Song, J.; Prox, M.; Weber, A.; Ehrenstein, G. W. In: Polypropylene: Structure, Blends; Composites; Karger-Kocsis, J., Ed.; Chapman & Hall: London, **1995;** p 273–294.
6. McHugh, A. J. *J. Appl. Polym. Sci.* **1975,** *19*, 125.
7. Southern, J. H.; Porter, R. S. *J. Appl. Polym. Sci.* **1970,** *14*, 2305.
8. Southern, J. H.; Porter R. S.; Bair H. E. *J. Polym. Sci.*, **1972**, 1135.
9. Hare, J. B.; Cucolo, J. A. *Midland Macromolecular Monographs (Flow-Induced Cryst. Polym. Syst.)* **1979,** *6*, 175.
10. Pornimit, B.; Ehrenstein, G. W. *Kunststoffe* **1989,** *79*, 43.
11. Pornimit, B.; Ehrenstein, G. W. *Adv. Polym. Technol.* **1992,** *11*, 91.
12. McHugh, A. J.; Tree, D. A.; Pornnimit, B.; Ehrenstein, G. W. *Int. Polym. Proc.* **1991,** *6*, 208.
13. Huang, H. X. *Polym. Eng. Sci.* **1998,** *38*, 1805.
14. Huang, H. X. *J. Mater. Sci. Lett.* **1999,** *18*, 225.
15. Ehrenstein, G. W.; Maertin, C. *Kunststoffe* **1985,** *75*, 20.
16. Pendse, A. V.; Collier, J. R. *J. Appl. Polym. Sci.* **1996,** *59*, 1305.
17. Obadal, M.; Čermák, R.; Stoklasa, K.; Habrová, V. *Plast. Rubber Compos.* **2004,** *33*, 295.
18. Čermák, R.; Obadal, M.; Habrová, V.; Stoklasa K.; Verney, V.; Commereuc, S.; Fraïsse, F. *Rheol. Acta* **2006,** *45*, 366–373.
19. Scherrer, P. In: X-Ray Diffraction Methods in Polymer Science; Alexander, L. E., Eds.; Wiley-Interscience: New York, **1969;** 582 p.
20. Wunderlich, B. Thermal Analysis; Academic Press: New York, **1990.**
21. Prox, M.; Pornnimit, B.; Varga, J.; Ehrenstein, G. W. *J. Thermal Anal.* **1990,** *36*, 1675.